I&EC research
Industrial & Engineering Chemistry Research

Article

Cite This: Ind. Eng. Chem. Res. 2017, 56, 14557−14564

pubs.acs.org/IECR

Process Synthesis and Optimization of Propylene/Propane Separation Using Vapor Recompression and Self-Heat Recuperation

Chang Chu En Christopher, Arnab Dutta, Shamsuzzaman Farooq, and Iftekhar A. Karimi*

Department of Chemical and Biomolecular Engineering, National University of Singapore, 4 Engineering Drive 4, Singapore 117585

Supporting Information

ABSTRACT: Propylene/propane separation is one of the most energy-intensive processes in the chemical industry. In this study, the concepts of mechanical vapor recompression (MVR) and self-heat recuperation (SHR) are simultaneously considered for the synthesis of four distillation-based configurations. Each configuration is optimized for the minimum total annualized separation cost using a simulation-based optimization framework with Aspen HYSYS as the process simulator and particle swarm optimization in MATLAB as the optimizer. The best configuration uses both MVR and SHR. MVR eliminates the need for reboiler steam, and SHR utilizes the remaining sensible heat to preheat the feed and the compressor inlet stream in MVR. This reduces the energy consumption by 45% and the separation costs by 20% as compared to the values for an MVR design with no SHR.

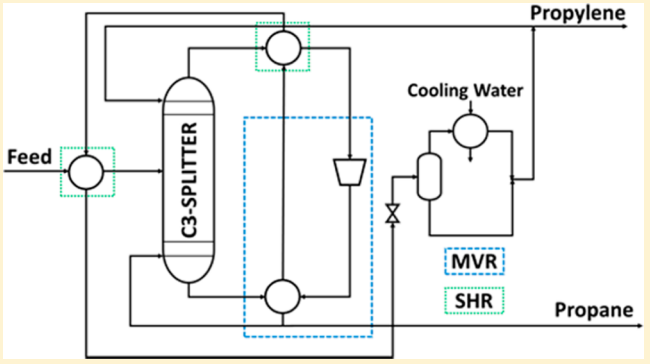

1. INTRODUCTION

Propylene is one of the most important petrochemicals produced globally today. Propylene is an essential raw material in the manufacture of a variety of propylene derivatives such as polypropylene, acrylonitrile, cumene, and acrylic acid. These derivatives are then processed to produce end products ranging from furniture, automobile parts, textiles, and packaging films to common household objects. Thus, it is evident that propylene is an important platform chemical. The global annual production capacity of propylene was estimated at 114 million tons in 2015, second behind ethylene among organic chemicals.[1] The global demand for propylene has been projected to rise faster than that of ethylene, growing at a rate of 5% annually.[2]

About 85% of the global propylene demand is met by conventional methods such as thermal cracking and fluid catalytic cracking.[1] Multiple hydrocarbon products, including light alkanes, alkenes, and aromatics, are generated through thermal cracking at high temperatures, and numerous separation steps are required before key products such as propylene and ethylene can be obtained. Other propylene production methods include on-purpose technologies (OPTs) such as propane dehydrogenation, olefin metathesis, and methanol-to-olefins and coal-to-olefins processes.[3] Propylene obtained from any of these sources is mixed with propane (and trace amounts of other hydrocarbons) and needs to be further purified for downstream applications. The manufacture of polypropylene, which accounts for about two-thirds of propylene consumption, requires polymer-grade propylene with a purity of 99.5% propylene by weight.[1] Thus, a C3 splitter (to separate propylene from propane) is almost inevitable in any propylene production unit.

According to the U.S. Department of Energy, the separation of propylene/propane mixtures by distillation is one of the most energy-intensive commercial distillation processes.[4,5] Separation of propylene/propane mixtures by distillation occurs either at high pressures (>20 bar) or at low pressures, where the latter requires cryogenic conditions.[6,7] At high pressures, the relative volatility of propylene and propane drops to about 1.08−1.12, depending on the mixture composition.[8] This results in high energy requirements at the reboiler, thus making this process highly energy-intensive. On the other hand, although the relative volatility of the components is considerably higher at lower pressures, the condenser needs to operate at cryogenic conditions to enable condensation of the top product. Among these two options, distillation at high pressure is generally favored from a cost perspective, because cooling water can be used as a cooling medium in the condenser, instead of refrigerants, which are expensive. Note that, as propylene and propane form a close-boiling mixture, C3 splitters can even require up to 240 stages for separation.[9,10]

The energy-intensive nature of propylene/propane separation has prompted researchers to explore alternative separation technologies such as extractive distillation,[11] membrane separation,[12,13] and adsorption.[4,14,15] There are also hybrid designs that combine different separation technologies, such as

Received: August 21, 2017
Revised: October 22, 2017
Accepted: November 16, 2017
Published: November 17, 2017

DOI: 10.1021/acs.iecr.7b03432
Ind. Eng. Chem. Res. 2017, 56, 14557−14564

hybrid membrane distillation,[12] hybrid adsorption distillation schemes,[16] and hybrid distillation−pervaporation schemes.[17] Eldridge presented an exhaustive review of different separation technologies that have been applied to olefin/paraffin mixtures such as propylene and propane.[18] Despite the proliferation of alternative separation technologies, distillation remains the primary means by which propylene and propane are separated in industry. Jana[19] and Kiss et al.[20] have presented excellent reviews of various energy-efficient distillation technologies for a variety of binary and multicomponent separation mixtures. Mechanical heat pumps (MHPs), which use electrical or mechanical energy to move heat from a heat source at a lower temperature to a heat sink at a higher temperature, have been successfully integrated with distillation columns, providing substantial energy savings without the need for major modifications to the existing process.[21] MHPs can be further broken down into three basic configurations: mechanical vapor recompression (MVR), external vapor recompression, and bottom flashing. Kazemi et al.[22] reduced the energy consumption of a benzene/toluene distillation process by modifying the conventional MVR design. Waheed et al.[23] enhanced the performance of a de-ethanizer unit by optimizing the MVR operating parameters. MVR has also been applied to processes such as desalination[24] and food product manufacturing.[25] Self-heat recuperation (SHR) is another energy-saving technology that can improve the energy efficiency of a process by circulating waste heat within the process streams to satisfy heating requirements. SHR has been applied to a variety of distillation processes including distillations of hydrocarbon systems,[26−28] crude oil distillation,[29] and cryogenic air separation,[30] each showing approximately 20−50% reduction in energy requirements. Internally heat integrated distillation columns (HIDiC), where heat transfer occurs directly between the stages in the stripping and rectification sections of a column, have also been extensively applied to energy-intensive processes such as propylene/propane separation.[9,31,32] However, HIDiC has not been implemented on an industrial-plant scale because of design and construction complexities.[19,33,34]

Recognizing the practical implementation issues with HIDiC that are yet to be fully resolved, the focus of this article is on MVR and SHR. It is evident from the open literature that MVR has been studied for the propylene/propane system. However, the synergistic effect of incorporating the concepts of MVR and SHR for a propylene/propane system has not yet been addressed. Thus, in this study, we propose different process configurations for a C3 splitter based on the concepts of MVR and SHR. We also optimize each of these proposed process configurations within a simulation-based optimization framework to obtain the configuration with the minimum separation cost for propylene.

2. PROCESS SYNTHESIS

2.1. Design Basis. According to the proprietary data from a local petrochemical company, a C3 splitter receives an 85:15 mol % liquid propylene/propane feed at 50 °C and 21 bar from the upstream C_3H_4 hydrogenation unit. The required specifications for the product streams from the C3 splitter are 99.6 wt % propylene purity (polymer-grade propylene[9]) with 99.0% recovery.[35] These result in a 95.0 wt % pure propane product (HD-5 propane[36]). The column uses a total condenser at 18 bar with 32 °C cooling water (CW) and a partial reboiler. A pressure drop of 0.7 kPa is assumed for each stage in the C3 splitter. Pressure drops across the condenser, reboiler, flash drums, and heat exchangers are all assumed to be zero. Therefore, the presence of several pumps (e.g., bottom of flash drums and condensers) and compressors common to all configurations is neglected. The minimum approach temperature for all heat exchangers is assumed to be 5 °C. Aspen HYSYS, version 9.0,[37] is used to simulate and evaluate alternate configurations for propylene/propane separation with the Peng−Robinson equation of state as the fluid package. The Peng−Robinson equation of state is appropriate for propylene/propane simulation as it shows a good fit between the experimental and simulation data.[38]

2.2. Configuration 1: Conventional Distillation. A high-pressure distillation column with CW as the coolant in the condenser is conventionally used in the industry for C3 splitting. Figure 1 shows the process flow diagram (PFD) for this configuration. With the column at 18 bar and 99.6% propylene purity, the number of stages (N_{DC}) and the feed stage location (F_{DC}) are the only decision variables available for optimizing this configuration.

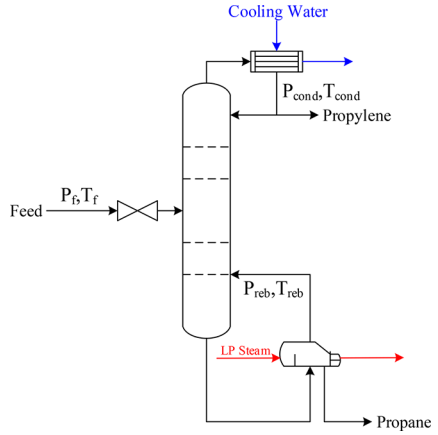

Figure 1. Configuration 1: Conventional distillation.

2.3. Configuration 2: Mechanical Vapor Recompression (MVR). MVR is a specific type of mechanical heat pump (MHP) system in which the process fluids (in this case, the top and bottom products of the C3 splitter) exchange heat with each other, as shown in Figure 2. The vapor stream from the column top at (P_t, T_t) undergoes compression, which increases its pressure and temperature to (P_1, T_1). The thermal energy (both latent and sensible) of this stream provides the reboiler heat with the condition that $T_1 > T_{reb}$. T_1 and the compressor

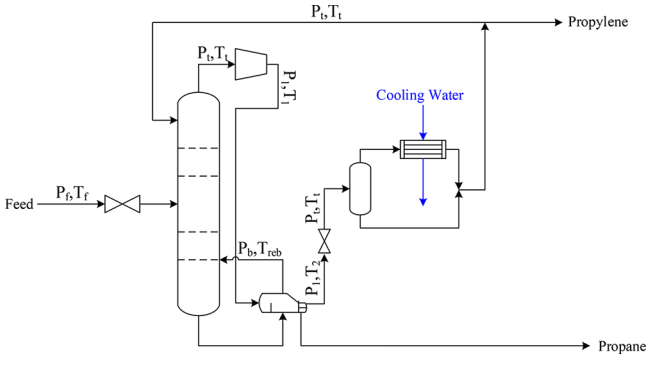

Figure 2. Configuration 2: Mechanical vapor recompression.

DOI: 10.1021/acs.iecr.7b03432
Ind. Eng. Chem. Res. 2017, 56, 14557−14564

power depend on the compressor pressure ratio $\left(\frac{P_1}{P_t}\right)$ and inlet vapor temperature (T_t). After supplying heat to the reboiler, the exit stream at (P_1, T_2) is expanded to P_t. This results in a two-phase mixture that is then separated in a flash drum, with the vapor being recondensed using CW before being mixed back with the liquid. A part of this liquid is removed as the propylene product, and the rest is used as reflux. Thus, N_{DC}, F_{DC}, and the compressor pressure ratio (P_{MVR}) are the decision variables for optimizing this configuration.

Now, we develop several modifications of configuration 2 and compare them with configuration 2. To make this comparison fair and simple, we fix the values N_{DC} and F_{DC} for all of the subsequent configurations (configurations 3, 4, and 5) at the values used for configuration 2.

2.4. Configuration 3: MVR with Compressor Inlet Preheating (CIP). In this configuration (Figure 3), the hot

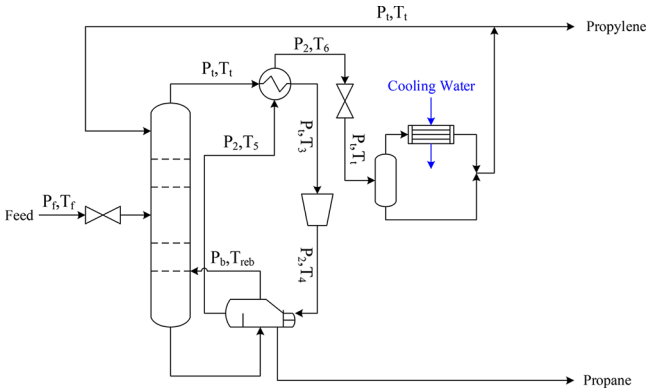

Figure 3. Configuration 3: Mechanical vapor recompression with compressor inlet preheating.

stream exiting the reboiler preheats the column vapor before the vapor is compressed (this is called compressor inlet preheating or CIP). Thus, the compressor pressure ratio (P_{MVR}) and compressor inlet temperature (T_{CIP}) are the decision variables for this configuration. The preheating of the column vapor gives it some of the heat it will eventually need for the reboiler. As the total reboiler duty remains the same, the compressor now needs to supply less energy to compress the column vapor. Therefore, the compressor needs a lower P_{MVR} compared to configuration 2 to satisfy the reboiler duty. This reduces the operating and capital costs of the compressor. Table 2 (below) lists the optimal P_{MVR} values for configurations 2−5, and one can see that P_{MVR} is indeed lower for configurations 3−5. The resultant cooled stream at (P_2, T_6) then follows the same processing steps as in configuration 2 to deliver liquid propylene.

2.5. Configuration 4: MVR with Feed Preheating. The sensible energy extracted from the reboiler exit stream in configuration 3 can also be used to preheat the feed to the distillation column, as shown in Figure 4. Note that both configurations 3 and 4 utilize the available sensible heat based on the concept of SHR. A preheated feed reduces the reboiler duty and lowers the compression ratio in comparison to that required for configuration 2. However, the pressure ratio is expected to be higher than that of configuration 3 because of the lower compressor inlet temperature. The upper limit set on the preheating is that the column feed must not be superheated vapor, which can lead to operating issues such as drying of the

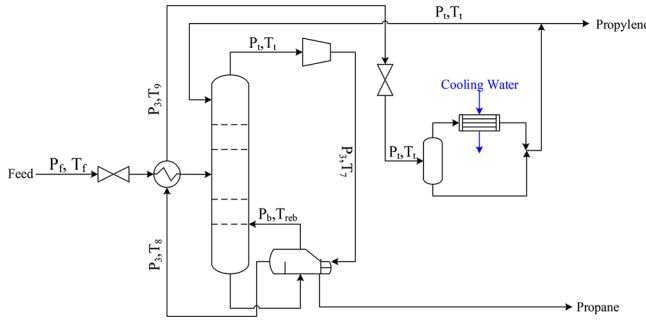

Figure 4. Configuration 4: Mechanical vapor recompression with feed preheating.

stripping section. Thus, P_{MVR} and the feed vapor fraction (q_{FP}) are the decision variables in the optimization of configuration 4.

2.6. Configuration 5: MVR with CIP and Feed Preheating. Configuration 5 (Figure 5) is obtained by

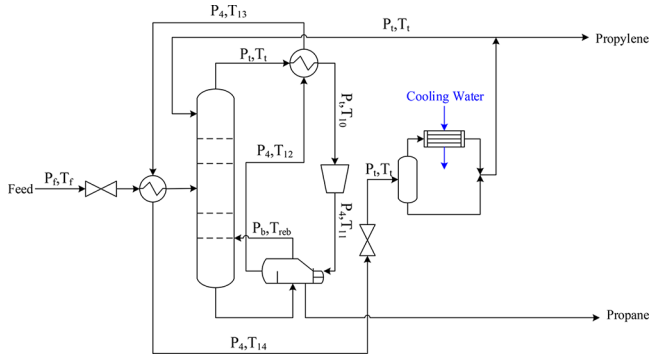

Figure 5. Configuration 5: Mechanical vapor recompression with compressor inlet and feed preheating.

combining configurations 3 and 4. The energy from the vapor stream exiting the compressor is first used to supply the reboiler duty, and then the sensible heat is used for CIP and finally for feed preheating. The rest of the process remains the same. Thus, P_{MVR}, T_{CIP}, and q_{FP} are the decision variables in the optimization of configuration 5.

3. PROCESS OPTIMIZATION

We minimize the total annualized cost (TAC) of separating propylene from propane by distillation for a given feed and product specifications as defined in the design basis according to the equation

$$\min \text{TAC (US\$/year)} = \text{OPEX} + f \times (\text{CAPEX}) \quad (1)$$

where OPEX is the operating cost per year and CAPEX is the total grassroots cost for the purchase and installation of all major equipment, updated to current-day prices using the Chemical Engineering Plant Cost Index (CEPCI) of 556.8 for January 2016.[39] Equation 2 defines the annualization factor, f, which is used to capitalize the investment cost over the plant equipment lifetime[42]

$$f = \frac{i(1+i)^n}{(1+i)^n - 1} \quad (2)$$

where i is fractional interest rate per year and n is the lifespan of plant equipment; 0.1 and 20 years are used as the values of i and n, respectively. Cost parameters and correlations for both

DOI: 10.1021/acs.iecr.7b03432
Ind. Eng. Chem. Res. 2017, 56, 14557−14564

OPEX and CAPEX follow the methodology as outlined by Turton et al.,[40] with the cost of electricity taken as $0.0723/kWh as obtained from the U.S. Energy Information Administration for the industrial sector in August 2016.[41] Note that each equipment unit has a specified range of sizes or capacities within which the cost correlations are valid, and outside the given ranges the cost estimates become inaccurate. To ensure that the cost correlations can be applied without violating the ranges specified by Turton et al.[40] the feed from the upstream process is split into identical parallel separation trains. Details about the costing methodology are provided in the Supporting Information.

3.1. Constraints. The constraints for the different configurations are listed in Table 1.

Table 1. Constraints for the Optimization Framework

variable	constrained value
propylene purity	99.6 wt %
propylene recovery	99.0%
minimum approach temperature for heat exchangers	≥5 °C
compressor	$1 < P_{MVR} < 4$
column feed	0 ≤ vapor fraction ≤ 1

3.2. Simulation-Based Optimization. Derivative-based optimization algorithms require accurate gradient information, which is not readily available from process simulators. Although derivatives for the variables can be indirectly obtained through perturbation, such an approach involves significantly longer computational times because the flowsheet within the process simulator needs to be solved each time a variable is perturbed. Moreover, the numerical noise inherent in process simulators affects the accuracy of computed derivatives.[43] These problems can be avoided through metaheuristic algorithms suitable for black-box optimization, where optimal solutions can be obtained through population-based search techniques without requiring any derivative information.[44] In metaheuristic algorithms, individuals in the population move within a predefined search space to locate the optimal solution.[43] In this study, particle swarm optimization (PSO) is selected as the optimization tool because of the relative ease of implementation, requiring only a few tuning parameters.[45] The PSO algorithm involves an element of learning and communication between particles (individuals) within the swarm (population), and the movement of each particle is governed by the respective best-known position and the best-known positions of the entire population. The entire swarm then gradually moves toward the optimal solution with each increasing iteration.[46,47] PSO effectively handles exploration and exploitation through the damping coefficient, w, which provides particles with a high velocity initially so that exploration of the search space can occur and later decreses the velocity to obtain solutions geared toward exploitation in the neighborhood of the optimal solution.[48] However, none of these metaheuristic algorithms can guarantee a global optimal solution.

A simulation-based optimization framework combines the benefits of using a process simulator, which seamlessly performs all thermodynamic calculations, with an external platform in which rigorous optimization algorithms can be implemented. In this work Aspen HYSYS as a process simulator is interfaced with MATLAB, version 2013b, as an external platform.[49] A connection between MATLAB and HYSYS can be established through a Component Object Model (COM) in ActiveX, which allows direct two-way communication between HYSYS and MATLAB.[50] As shown in Figure 6, stream and process data

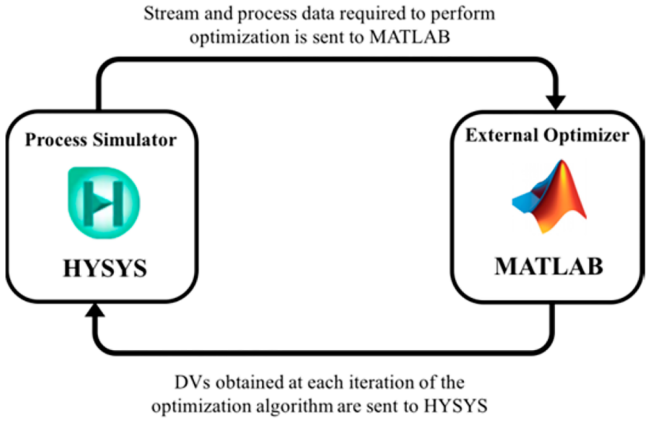

Figure 6. HYSYS–MATLAB interface.

obtained from HYSYS are sent to MATLAB, which performs the optimization, and the decision variables obtained at each iteration of the optimization are sent back to HYSYS to perform the process simulation.

An overview of our optimization algorithm is provided in Figure 7. N_{DC} and F_{DC} are the discrete decision variables for the distillation column. We optimize these variables for configurations 1 and 2 as follows: We fix the continuous variables (P_{MVR}, T_{CIP}, q_{FP}) at some nominal values and then compute the total annualized cost for each possible combination of N_{DC} and F_{DC}. We choose the combination with the minimum cost. Once we have determined the best N_{DC} and F_{DC} values for configuration 2, we then use the same values for configurations 3–5, so no discrete optimization is needed for these configurations.

For the optimization of the continuous variables, we use the PSO algorithm. A key parameter in the PSO framework is the population size or the number of particles in a swarm. A series of computational trials is performed to analyze the trade-off between computational time and objective-function value. As population size increases, the optimal solution improves marginally, but the computational time increases significantly because more function evaluations must be performed. The number of iterations is another key parameter, because PSO involves a social learning component that updates the movement of the particles toward the best solution obtained for each iteration. As the number of iterations increase, the solutions gradually converge to the optimal solution. A population size of 15 particles with a maximum number of iterations of 20 is used for all simulations reported in this study. The PSO is initialized by assigning each particle a random position within the predefined search space bounded by the ranges of the decision variables. The objective function is then evaluated for each particle. Equation 1 has been modified to include a penalty term to handle constraint violations, as shown in the equation

$$\min \mathrm{TAC}\left(\frac{\mathrm{US\$}}{\mathrm{year}}\right) = \mathrm{OPEX} + f \times (\mathrm{CAPEX}) + z \tag{3}$$

The penalty parameter (z) is of the same order of magnitude as the other terms in eq 3.

DOI: 10.1021/acs.iecr.7b03432
Ind. Eng. Chem. Res. 2017, 56, 14557–14564

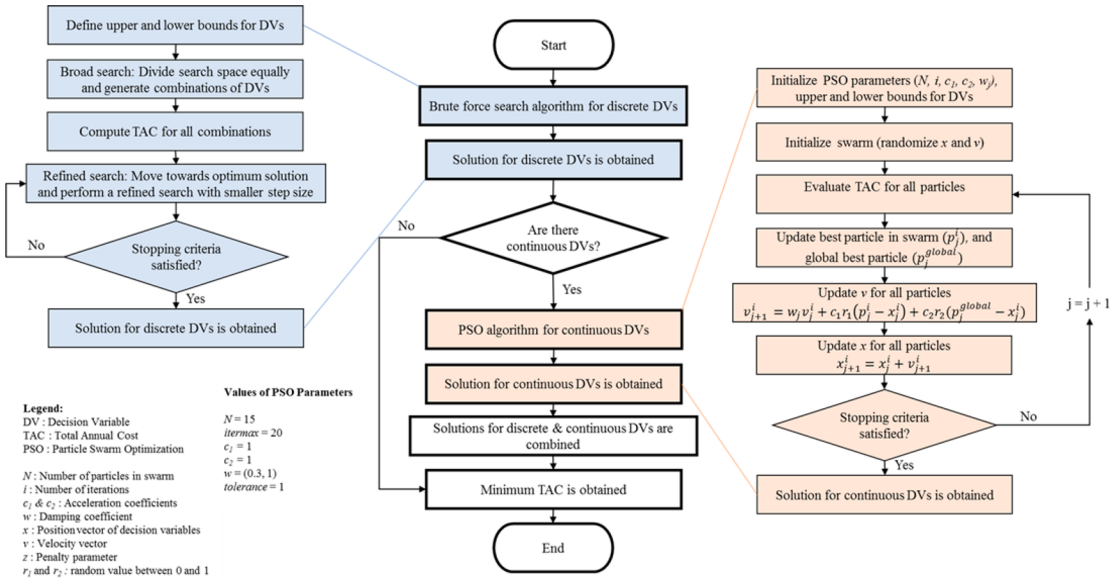

Figure 7. Optimization framework.

Table 2. Comparison of All Five Configurations for Producing 0.45 MTPA of Propylene

	configuration				
	1	2	3	4	5
no. of stages	240	147	147	147	147
feed stage	176	98	98	98	98
compression ratio (P_{MVR})	–	2.15	1.52	1.65	1.49
compressor inlet temperature (°C) (T_{CIP})	–	44.0	54.0	44.0	48.0
feed vapor fraction (q_{FP})	0.03	0.03	0.03	1.0	1.0
MVR power consumption (MW)	–	14.6	8.8	9.7	8.1
thermal energy requirement (GJ/h)	260.3	–	–	–	–
thermal energy equivalent of electricity consumed in MVR–SHR (GJ/h)	–	157.7	95.0	104.8	87.5
total annualized cost (10^6 US$/year)	36.1	20.4	17.5	16.8	16.4
propylene separation cost (US$/ton)	80.2	45.2	38.9	37.3	36.3

The velocity and position of each particle are updated according to the equations given in Figure 7, which considers both the best-known positions of the individual particles and the best-known positions of the entire population. At each iteration, the algorithm updates the best-known position of a particle if a better position is obtained; otherwise, it retains the previous best position, and the particle with the minimum function value is considered as the best particle within the entire population. This iterative process continues until a specified termination criterion is met. The terminations of both the exhaustive search and PSO optimization algorithms require appropriate stopping criteria.[51] The exhaustive search is terminated when all combinations of the two discrete variables within the search space have been exhausted. For PSO, we use a distribution-based criterion, in which the algorithm is terminated if the objective-function values for the best and worst particles do not differ by more than a threshold in any iteration or the limit on the maximum number of iterations has been reached.

4. TECHNOECONOMIC ANALYSIS

For configuration 1, TAC decreases monotonically with N_{DC}, whereas a U-shaped trend is observed for TAC when F_{DC} is varied. This is caused by the variation in the reflux ratio as F_{DC} changes. Φ, a dimensionless variable indicating the relative position of the feed stage within the column, is defined as

$$\Phi = F_{DC}/N_{DC} \quad (4)$$

Based on the trends in N_{DC} and F_{DC}, the search space for configuration 1 is constrained to the ranges 200–240 and 0.4–0.8 for N_{DC} and Φ, respectively. The optimal column design for configuration 1 has 240 stages with the feed stage at stage 176 (from the top).

When MVR is incorporated into the design, a trend of TAC increasing with N_{DC} is observed, because consumption of steam in the reboiler is eliminated. As a result, TAC for configuration 2 is dominated by capital cost. Among the components of the capital cost, column cost is the most significant. The total cost of the column trays and the total volume of the column are directly proportional to N_{DC}; therefore, total capital cost decreases as N_{DC} decreases. The search space for the optimization of configuration 2 is constrained to the ranges 140–200 and 0.4–0.8 for N_{DC} and Φ, respectively. Beyond the lower bound of N_{DC}, the specifications for propylene purity and recovery can no longer be achieved. The optimal column design for configuration 2 has 147 stages with the feed stage at stage 98 (from the top). The solution for the discrete variables, N_{DC} and F_{DC}, that are obtained for configuration 2 are also applied to configurations 3–5.

DOI: 10.1021/acs.iecr.7b03432
Ind. Eng. Chem. Res. 2017, 56, 14557–14564

Because it is stochastic in nature, PSO does not guarantee that the same optimal solution will be obtained each time PSO is executed.[43,52] The objective function, being nonlinear in nature, results in slightly different combinations of decision variables to give solutions with similar objective-function values. Thus, PSO is repeated multiple times to ascertain the validity of the optimal solution. More information on the performance of the PSO algorithm is available in the Supporting Information.

Table 2 presents the optimized results obtained for all configurations. For configuration 1, the operating costs strongly influence the TAC, whereas for the rest of the configurations (configurations 2−5), the annualized capital cost is dominant owing to a reduction of 65−81% in operating costs as the heat recovered through MVR completely satisfies the reboiler duty, thus eliminating the requirement for steam. The TAC of the basic MVR design in configuration 2 is further reduced by incorporating CIP, feed preheating, and a combination of both CIP and feed preheating into configurations 3, 4, and 5, respectively. In addition to the cost savings obtained from configuration 2, these modifications resulted in further reductions of 14−20% in the TAC. In configuration 3, an increase in the fluid temperature at the compressor inlet through the use of CIP results in a reduction in the compressor power requirement compared to that of configuration 2. Implementing the concept of feed preheating in configuration 4 shifts a part of the reboiler duty, which is used to vaporize the liquid within the column, to the feed preheater. The feed preheater utilizes the sensible heat (after the required energy has been supplied to the reboiler) to increase the enthalpy of the feed stream. This leads to a reduction in reboiler duty, so that less energy is to be recovered through MVR. This ultimately leads to a reduction in the compressor power requirement compared to that of configuration 2. Configuration 5 makes use of the high-enthalpy stream generated from MVR to sequentially transfer heat between the process streams. It reaps reductions in TAC coming from the CIP as well as the feed preheating and proves to be the best configuration from the perspectives of both energy and costs. Configuration 5 leads to reductions of 45% in the energy consumption for the propylene/propane separation process and 20% in the separation cost as compared to the values for the MVR design with no SHR (configuration 2). The electricity demands of MVR for configurations 2−5 are also converted to a thermal energy basis by assuming a 33% efficiency for obtaining electricity from thermal energy through the combustion of fuels.[53] The thermal energy equivalents of electricity consumption for all five configurations are presented in Table 2.

5. CONCLUSIONS

In this study, four different distillation-based configurations employing various combinations of mechanical vapor recompression and self-heat recuperation are proposed, optimized, and compared in terms of their abilities to reduce the energy consumption of a C3 splitter. The two techniques fully eliminate the need for low-pressure steam in the reboiler and reduce the total energy consumption and separation cost. The best configuration employs both mechanical vapor recompression and self-heat recuperation and reduces the annualized separation cost by 20% and the energy consumption by 45%, when compared to the configuration with simple mechanical vapor recompression alone. The modifications proposed in this study for the mechanical vapor recompression system can also reduce the costs and energy consumptions for other energy-intensive distillation processes.

■ ASSOCIATED CONTENT

Supporting Information

The Supporting Information is available free of charge on the ACS Publications website at DOI: 10.1021/acs.iecr.7b03432.

Stream data for optimal configurations, costing methodology, and PSO algorithm results (PDF)

■ AUTHOR INFORMATION

Corresponding Author

*E-mail: cheiak@nus.edu.sg. Tel.: +65 6516-6359.

ORCID

Shamsuzzaman Farooq: 0000-0002-6501-5540

Iftekhar A. Karimi: 0000-0001-7122-0578

Notes

The authors declare no competing financial interest.

■ ACKNOWLEDGMENTS

We acknowledge AspenTech Inc. for allowing the use of HYSYS under an academic license provided to the National University of Singapore. We also acknowledge MathWorks for providing an academic license for MATLAB to the National University of Singapore. A.D. thanks the Department of Chemical and Biomolecular Engineering, NUS, for providing NUS Research Scholarship (NRS). We also acknowledge Mr. Kuah Wee Chong for his input at different stages of this work.

■ NOMENCLATURE

Abbreviations

CAPEX = capital cost (US$/year)
CIP = compressor inlet preheating
DV = decision variable
MHP = mechanical heat pump
MVR = mechanical vapor recompression
OPEX = operating cost (US$/year)
PSO = particle swarm optimization
SHR = self-heat recuperation
TAC = total annualized cost (US$/year)

Symbols

f = annualization factor
F_{DC} = feed stage location from the top of the distillation column
h = stream enthalpy
i = fractional interest rate per year
n = number of years
N_{DC} = number of stages in the distillation column
P_i = pressure of stream i
P_{MVR} = compression ratio of the MVR compressor
q_{FP} = vapor fraction of the feed stream entering the distillation column
T_{CIP} = temperature of the suction stream to the MVR compressor
T_i = temperature of stream i
z = penalty parameter

Greek Symbols

Φ = dimensionless feed stage location

Subscripts

cond = condenser

DOI: 10.1021/acs.iecr.7b03432
Ind. Eng. Chem. Res. 2017, 56, 14557−14564

reb = reboiler

REFERENCES

(1) Coombs, D. Propylene: The "Other" Olefin. Presented at the *Goldman Sachs Chemical Intensity Conference*, Houston, TX, Mar 15, 2016.

(2) Horncastle, A.; Gotpagar, J.; Ozeir, F.; Singh, S. *Global Petrochemical Disruptions: Business Model Innovations for a Dynamic Market*; Strategy&: New York, 2014.

(3) Moulijn, J. A.; Makkee, M.; van Diepen, A. E. *Chemical Process Technology*, 2nd ed.; John Wiley & Sons: Chichester, U.K., 2013.

(4) Jarvelin, H.; Fair, J. R. Adsorptive Separation of Propylene−Propane Mixtures. *Ind. Eng. Chem. Res.* **1993**, *32* (10), 2201.

(5) Ghosh, T. K.; Lin, H. Da; Hines, A. L. Hybrid Adsorption-Distillation Process for Separating Propane and Propylene. *Ind. Eng. Chem. Res.* **1993**, *32* (10), 2390.

(6) Alcántara-Avila, J. R.; Gómez-Castro, F. I.; Segovia-Hernández, J. G.; Sotowa, K. I.; Horikawa, T. Optimal Design of Cryogenic Distillation Columns with Side Heat Pumps for the Propylene/propane Separation. *Chem. Eng. Process.* **2014**, *82*, 112.

(7) Baker, R. W. Future Directions of Membrane Gas Separation Technology. *Ind. Eng. Chem. Res.* **2002**, *41*, 1393.

(8) Mann, A. N.; Pardee, W. A.; Smyth, R. W. Vapor-Liquid Equilibrium Data for Propylene-Propane System. *J. Chem. Eng. Data* **1963**, *8* (4), 499.

(9) Olujić, Ž.; Sun, L.; de Rijke, A.; Jansens, P. J. Conceptual Design of an Internally Heat Integrated Propylene-Propane Splitter. *Energy* **2006**, *31* (15), 3083.

(10) Olujic, Z.; Fakhri, F.; De Rijke, A.; De Graauw, J.; Jansens, P. J. Internal Heat Integration - The Key to an Energy-Conserving Distillation Column. *J. Chem. Technol. Biotechnol.* **2003**, *78* (2−3), 241.

(11) Liao, B.; Lei, Z.; Xu, Z.; Zhou, R.; Duan, Z. New Process for Separating Propylene and Propane by Extractive Distillation with Aqueous Acetonitrile. *Chem. Eng. J.* **2001**, *84* (3), 581.

(12) Benali, M.; Aydin, B. Ethane/ethylene and Propane/propylene Separation in Hybrid Membrane Distillation Systems: Optimization and Economic Analysis. *Sep. Purif. Technol.* **2010**, *73* (3), 377.

(13) Pan, Y.; Li, T.; Lestari, G.; Lai, Z. Effective Separation of Propylene/propane Binary Mixtures by ZIF-8 Membranes. *J. Membr. Sci.* **2012**, *390−391*, 93.

(14) Bao, Z.; Alnemrat, S.; Yu, L.; Vasiliev, I.; Ren, Q.; Lu, X.; Deng, S. Adsorption of Ethane, Ethylene, Propane, and Propylene on a Magnesium-Based Metal-Organic Framework. *Langmuir* **2011**, *27* (22), 13554.

(15) Khalighi, M.; Karimi, I. A.; Farooq, S. Comparing SiCHA and 4A Zeolite for Propylene/propane Separation Using a Surrogate-Based Simulation/optimization Approach. *Ind. Eng. Chem. Res.* **2014**, *53* (44), 16973.

(16) Kumar, R.; Golden, T. C.; White, T. R.; Rokicki, A. Novel Adsorption Distillation Hybrid Scheme for Propane/Propylene Separation. *Sep. Sci. Technol.* **1992**, *27* (15), 2157.

(17) Naidu, Y.; Malik, R. K. A Generalized Methodology for Optimal Configurations of Hybrid Distillation-Pervaporation Processes. *Chem. Eng. Res. Des.* **2011**, *89* (8), 1348.

(18) Eldridge, R. B. Olefin/Paraffin Separation Technology: A Review. *Ind. Eng. Chem. Res.* **1993**, *32*, 2208.

(19) Jana, A. K. Advances in Heat Pump Assisted Distillation Column: A Review. *Energy Convers. Manage.* **2014**, *77*, 287.

(20) Kiss, A. A.; Flores Landaeta, S. J.; Infante Ferreira, C. A. Towards Energy Efficient Distillation Technologies - Making the Right Choice. *Energy* **2012**, *47* (1), 531.

(21) Annakou, O.; Mizsey, P. Rigorous Investigation of Heat Pump Assisted Distillation. *Heat Recovery Syst. CHP* **1995**, *15* (3), 241.

(22) Kazemi, A.; Hosseini, M.; Mehrabani-Zeinabad, A.; Faizi, V. Evaluation of Different Vapor Recompression Distillation Configurations Based on Energy Requirements and Associated Costs. *Appl. Therm. Eng.* **2016**, *94*, 305.

(23) Waheed, M. A.; Oni, A. O.; Adejuyigbe, S. B.; Adewumi, B. A.; Fadare, D. A. Performance Enhancement of Vapor Recompression Heat Pump. *Appl. Energy* **2014**, *114*, 69.

(24) Aly, N. H.; El-Figi, A. K. Mechanical Vapor Compression Desalination Systems - A Case Study. *Desalination* **2003**, *158* (1−3), 143.

(25) Chua, K. J.; Chou, S. K.; Yang, W. M. Advances in Heat Pump Systems: A Review. *Appl. Energy* **2010**, *87* (12), 3611.

(26) Van Duc Long, N.; Lee, M. A Novel NGL (Natural Gas Liquid) Recovery Process Based on Self-Heat Recuperation. *Energy* **2013**, *57*, 663.

(27) Matsuda, K.; Kawazuishi, K.; Kansha, Y.; Fushimi, C.; Nagao, M.; Kunikiyo, H.; Masuda, F.; Tsutsumi, A. Advanced Energy Saving in Distillation Process with Self-Heat Recuperation Technology. *Energy* **2011**, *36* (8), 4640.

(28) Kiuchi, T.; Yoshida, M.; Kato, Y. Energy Saving Bioethanol Distillation Process with Self-Heat Recuperation Technology. *J. Jpn. Pet. Inst.* **2015**, *58* (3), 135.

(29) Kansha, Y.; Kishimoto, A.; Tsutsumi, A. Application of the Self-Heat Recuperation Technology to Crude Oil Distillation. *Appl. Therm. Eng.* **2012**, *43*, 153.

(30) Fu, Q.; Kansha, Y.; Song, C.; Liu, Y.; Ishizuka, M.; Tsutsumi, A. A Cryogenic Air Separation Process Based on Self-Heat Recuperation for Oxy-Combustion Plants. *Appl. Energy* **2016**, *162*, 1114.

(31) Shahandeh, H.; Ivakpour, J.; Kasiri, N. Feasibility Study of Heat-Integrated Distillation Columns Using Rigorous Optimization. *Energy* **2014**, *74* (C), 662.

(32) Nakaiwa, M.; Huang, K.; Endo, a.; Ohmori, T.; Akiya, T.; Takamatsu, T. Internally Heat-Integrated Distillation Columns: A Review. *Chem. Eng. Res. Des.* **2003**, *81* (1), 162.

(33) Chen, H.; Huang, K.; Wang, S. A Novel Simplified Configuration for an Ideal Heat-Integrated Distillation Column (Ideal HIDiC). *Sep. Purif. Technol.* **2010**, *73* (2), 230.

(34) Harwardt, A.; Marquardt, W. Heat-Integrated Distillation Columns: Vapor Recompression or Internal Heat Integration? *AIChE J.* **2012**, *58* (12), 3740.

(35) Wu, W.; Shao, B.; Zhou, X. Dynamic Control of a Selective Hydrogenation Process with Undesired MAPD Impurities in the C3-Cut Streams. *J. Taiwan Inst. Chem. Eng.* **2015**, *54*, 28.

(36) Bryan, P. F. Removal of Propylene from Fuel-Grade Propane. *Sep. Purif. Rev.* **2004**, *33* (2), 157.

(37) *Aspen HYSYS for Hydrocarbons*; AspenTech Inc.:Cambridge, MA, 2016. http://www.aspentech.com/products/aspen-hysys/ (accessed Dec 22, 2016).

(38) Pandey, S. *Simulation and Mulitobjective Optimization of Cold-End Separation Process in an Ethylene Plant*. Master's Thesis, National University of Singapore, Singapore, 2013.

(39) Jenkins, S. Current Economic Trends - March 2016, Access Intelligence, LLC, Rockville, MD, 2016. http://www.chemengonline.com/current-economic-trends-march-2016/?printmode=1 (accessed Nov 28, 2016).

(40) Turton, R.; Bailie, R. C.; Whiting, W. B.; Shaewitz, J. A.; Bhattacharya, D. *Analysis Synthesis and Design of Chemical Processes*, 4th ed.; Prentice Hall International Series in the Physical and Chemical Engineering Sciences; Prentice Hall: Ann Arbor, MI, 2012.

(41) Average Price of Electricity to Ultimate Customers by End-Use Sector, by State, August 2016 and 2015 (Cents per Kilowatthour). U.S. Energy Information Administration, Washington, DC, 2016. http://www.eia.gov/electricity/monthly/epm_table_grapher.cfm?t=epmt_5_6_a (accessed Nov 28, 2016).

(42) Smith, R. *Chemical Process: Design and Integration*; John Wiley & Sons, Ltd: Chichester, U.K., 2005.

(43) Javaloyes-Antón, J.; Ruiz-Femenia, R.; Caballero, J.a. Rigorous Design of Complex Distillation Columns Using Process Simulators and the Particle Swarm Optimization Algorithm. *Ind. Eng. Chem. Res.* **2013**, *52* (44), 15621.

(44) Adams, T. A.; Seider, W. D. Practical Optimization of Complex Chemical Processes with Tight Constraints. *Comput. Chem. Eng.* **2008**, *32* (9), 2099.

DOI: 10.1021/acs.iecr.7b03432
Ind. Eng. Chem. Res. 2017, 56, 14557−14564

(45) Khan, M. S.; Lee, M. Design Optimization of Single Mixed Refrigerant Natural Gas Liquefaction Process Using the Particle Swarm Paradigm with Nonlinear Constraints. *Energy* **2013**, *49* (1), 146.
(46) Eberhart, R.; Kennedy, J. A New Optimizer Using Particle Swarm Theory. *Proc. Sixth Int. Symp. Micro Mach. Hum. Sci.* **1995**, 39.
(47) Eberhart, R. C.; Shi, Y. Particle Swarm Optimization: Developments, Applications and Resources. *Proc. of the 2001 Congress on Evolutionary Computation IEEE Press* **2001**, 81.
(48) Kim, M. J.; Song, H.-Y.; Park, J.-B.; Roh, J.-H.; Lee, S. U.; Son, S.-Y. An Improved Mean-Variance Optimization for Nonconvex Economic Dispatch Problems. *J. Electr. Eng. Technol.* **2013**, *8* (1), 80.
(49) *MATLAB*, version 2013b; The MathWorks, Inc.: Natick, MA, 2013. https://www.mathworks.com/products/matlab.html (accessed Jan 6, 2017).
(50) Navarro-Amorós, M. a.; Ruiz-Femenia, R.; Caballero, J. a. Integration of Modular Process Simulators under the Generalized Disjunctive Programming Framework for the Structural Flowsheet Optimization. *Comput. Chem. Eng.* **2014**, *67*, 13.
(51) Zielinski, K.; Laur, R. Stopping Criteria for a Constrained Single-Objective Particle Swarm Optimization Algorithm. *Informatica* **2007**, *31* (1), 51.
(52) Brits, R.; Engelbrecht, A. P.; van den Bergh, F. Locating Multiple Optima Using Particle Swarm Optimization. *Appl. Math. Comput.* **2007**, *189* (2), 1859.
(53) Kiran, B.; Jana, A. K.; Samanta, A. N. A Novel Intensified Heat Integration in Multicomponent Distillation. *Energy* **2012**, *41* (1), 443.

DOI: 10.1021/acs.iecr.7b03432
Ind. Eng. Chem. Res. 2017, 56, 14557−14564